International Journal of Heat and Mass Transfer 55 (2012) 2204–2207

Contents lists available at SciVerse ScienceDirect

International Journal of Heat and Mass Transfer

journal homepage: www.elsevier.com/locate/ijhmt

Technical Note

# Operational characteristics of two biporous wicks used in loop heat pipe with flat evaporator

B.B. Chen, Z.C. Liu *, W. Liu *, J.G. Yang, H. Li, D.D. Wang

*School of Energy and Power Engineering, Huazhong University of Science and Technology, Wuhan 430074, China*

ARTICLE INFO

*Article history:*
Received 1 August 2011
Received in revised form 23 November 2011
Accepted 28 November 2011
Available online 27 December 2011

*Keywords:*
Biporous wick
Loop heat pipe
Flat evaporator
Heat flux
Electronic cooling

ABSTRACT

Two special biporous wicks are adopted in stainless-steel–ammonia loop heat pipes (LHPs) with flat evaporator to enhance their heat transfer performances. The experimental results demonstrate that thermal and hydraulic characteristics of the wick with porosity of 69% (in LHP 2) are better than that of the wick with porosity of 65% (in LHP 1). The maximum heat loads of LHP 1 and LHP 2 could, respectively, reach 120 W (heat flux 11.8 W/cm$^2$) and 130 W (12.8 W/cm$^2$) at the allowable evaporator temperature below 60 °C. Meanwhile, they can start up at heat load as low as 2.5 W. The LHPs show very fast and smooth response to heat load and operate stably without obvious temperature oscillation. The total thermal resistances of the LHPs vary between 1.47 and 0.33 °C/W at heat load ranging from 10 to 130 W.



## 1. Introduction

In recent decades, loop heat pipe (LHP) has raised scholars' interests in thermal control of compact electronic devices with high heat flux and limited space. LHP is an efficient two-phase device and possesses all the advantages of conventional heat pipe and additionally include simple structure, flexible transport lines and heat transfer over long distances. Many scholars and researchers have studied the operating principle of LHP experimentally and theoretically [1–3]. The evaporators are usually designed into cylinder or plate shapes among all the existing LHP devices. Flat evaporator has some advantages of flat thermo-contact surface, high isothermality, low thermal resistance and small mass of the body. So it is very suitable for compact electronic equipment which needs large quantity of heat to dissipate.

Experimental investigations [4–8] on LHP with flat evaporator were carried out to improve their heat transfer performances. The experimental results showed that some parameters including the configuration of flat evaporator, fluid inventory, the working fluid, elevation, the wick structure, heat sink temperature and non-condense gases (NCGs) had influences on the start-up and operation of the LHPs. Although the LHPs could start up and operate in a certain heat load range, the evaporator temperatures are too high at high heat flux. They are limited to apply to heat dissipation in the electronic equipment. Among the components of the LHP, the wick structure is very critical for it. A special wick structure, biporous wick with various bimodal pore size distributions, was investigated by many researchers [9–11]. The study indicated that the biporous wick has advantage for solving the limitation of drying out in the wick structure at high heat flux. Although much work has been noted that biporous wick could improve the heat transfer performance for heat pipes, there are rare literatures about biporous wick used in the LHP with flat evaporator.

In this work, two special biporous wicks were used in the flat evaporators and 60 °C was set as the typical maximum allowed evaporator temperature for electronic equipment in our original intention. The goals of this investigation were to compare the thermophysical and hydraulic characteristics of the two biporous wicks with different parameters used in LHP and to reveal the detailed characteristics of the LHP with flat evaporator during start-up and steady operation.

## 2. Experimental setup

### 2.1. Fabrication of the biporous wick structure

There are two methods to manufacture wick structure with bimodal pore size distributions: bidispersed wick and biporous wick, which are introduced in detail in Ref. [9]. In this study, the wicks were fabricated by the latter method. The detailed structure of the biporous wick is shown in Ref. [11]. The large pores reduce the flow resistance and enhance the liquid transport and the vapor

* Corresponding authors. Address: 415 Power Building, 1037 Luoyu Road, Hongshan District, Wuhan 430074, China. Tel.: +86 27 87542618; fax: +86 27 87540724.

*E-mail addresses:* zcliu@hust.edu.cn (Z.C. Liu), w_liu@hust.edu.cn (W. Liu).

0017-9310/$ - see front matter 
doi:10.1016/j.ijheatmasstransfer.2011.12.004

**Nomenclature**

| | |
|---|---|
| $Q$ | heat load (W) |
| $R$ | thermal resistance (°C/W) |
| $T$ | temperature (°C) |

*Subscripts*

| | |
|---|---|
| cond | condenser |
| evap | evaporator |
| sink | heat sink |

*Abbreviations*

| | |
|---|---|
| Amb | the ambient air |
| CC | compensation chamber |
| TC | thermocouple |

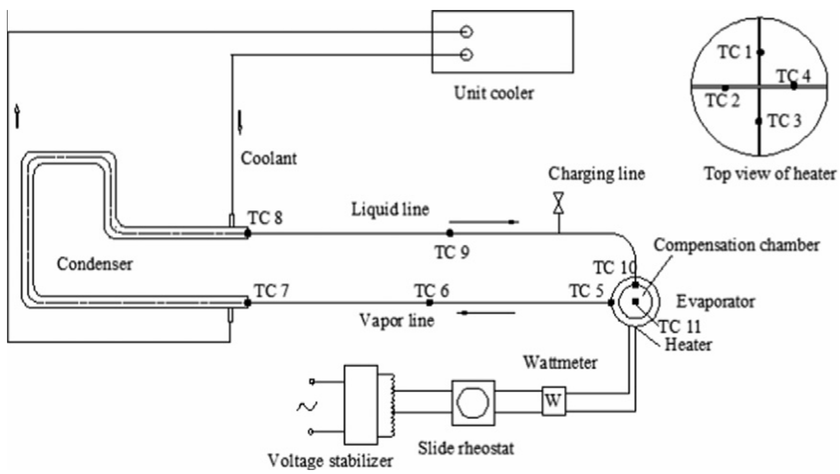


**Fig. 1.** The design and test schematic of the experimental prototype.

escape from the wick. The small pores continue to function as liquid supply pump developing the capillary force. Also, the biporous wick increases the evaporating surface area. So the bimodal pore size distributions allow the biporous wick to yield excellent hydrodynamic performance.

Porosity and permeability are measured by experimental methods [10,12]. The uncertainty analyses of the porosity and permeability are estimated to be within ±0.64% and ±8.4% respectively. The effective pore radius and the pore size distribution are analyzed using the image analysis method in the present study.

*2.2. LHP prototype and test method*

Fig. 1 shows the design schematic of the LHP prototype and the experimental test setups. A double-pipe heat exchanger is designed as the condenser. A charging line is fixed on the liquid line for creating a vacuum and charging the working fluid. The condenser and the liquid line are insulated using efficient thermal insulation material. Two LHP prototypes using different biporous wicks are fabricated and the relative error of fabrication is less than 5%. Table 1 presents the main parameters of the LHPs. The working fluid is not added to the loop until no leak is detected. Ammonia is used as the working fluid and the liquid charge ratio is selected at 65%.

The heat simulator (active area 10.2 cm$^2$) is a cooper block heated with three embedded cartridge heaters. A 10 mm thick nano-adiabatic material is used to insulate the heat simulator. Heat loss to the ambient is estimated to be less than 0.5% of the input power. And a slide rheostat connected with the wattmeter with a relative error of 0.5% and the voltage stabilizer is used to control the input power. The accuracy of $T$-type thermocouple is ±0.2 °C. The locations of the thermocouples are showed in Fig. 1. The evaporator temperature is presented by the temperature measured at the cross groove of the heater wall. The LHPs are tested in the horizontal orientation.

**Table 1**
The main geometrical parameters of the LHPs.

| Porous wick | LHP 1<br>Sample 1 | LHP 2<br>Sample 2 |
|---|---|---|
| Diameter (mm) | 36.3 | 37 |
| Thickness (mm) | 3.7 | 4 |
| Porosity (%) | 65 | 69 |
| Permeability (m$^2$) | $6.3 \times 10^{-13}$–$6.6 \times 10^{-13}$ | $1.0 \times 10^{-12}$–$1.4 \times 10^{-12}$ |
| Porous radius (μm) | 2.6–53 | 2.6–53 |
| Evaporator diameter (mm) | 43 | 43 |
| Evaporator thickness (mm) | 15 | 15 |
| CC diameter (mm) | 40 | 40 |
| Vapor line length (mm) | 340 | 335 |
| Liquid line length (mm) | 400 | 415 |
| Condenser length (mm) | 920 | 960 |

## 3. Results and discussions

*3.1. Start-up tests*

Start-up behavior of the LHP is an important aspect to evaluate its reliability and stability. Fig. 2 shows the start-up process of the LHP 1 with a heat load of 100 W at the heat sink temperature of −15 °C. As soon as input power is applied to the evaporator active zone, temperatures of the evaporator wall, the evaporator outlet and the condenser inlet increase quickly. At the same time, the condenser outlet temperature has a stepwise decrease. That means the liquid inside the evaporator starts evaporating. When the vapor accumulates more, the evaporating meniscus is formed on the

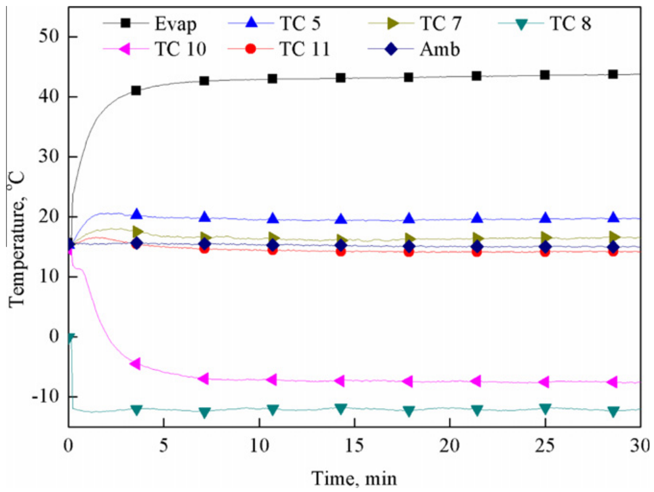


**Fig. 2.** Start-up process of the LHP 1 with 100 W at the heat sink temperature of −15 °C.

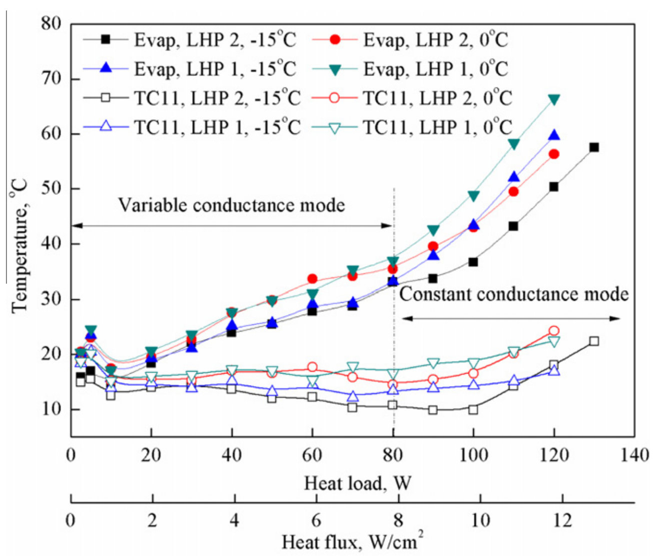


**Fig. 3.** Evaporator and CC temperatures of the LHPs at the heat sink temperatures of −15 and 0 °C.

interface of the biporous wick. The circulation is not formed until the capillary force is larger than the total pressure drops in the system. The liquid subcooled in the condenser flows towards the CC. So the evaporator inlet temperature begins to decrease. The CC temperature is decided by heat exchange with the evaporator, the ambient, and the liquid returning from the condenser [3]. The LHP will reach steady state when energy balances for all the loop elements are satisfied. At last, the capillary force is equal to the total pressure drops. The whole processes are very smoothly and no obvious temperature oscillation phenomena are observed. It should be mentioned that no obvious temperature oscillation were observed in all tests of LHP 1 and LHP 2.

### 3.2. Operating characteristic of LHP

The temperature indicated in the following are measured at steady state. Fig. 3 presents the evaporator and the CC temperatures of LHP 1 and LHP 2 at two heat sink temperatures. The LHPs are able to start up at heat load as low as 2.5 W. The maximum heat load which the LHP 1 and the LHP 2 could transfer, respectively, reaches 120 W (heat flux 11.8 W/cm$^2$) and 130 W (12.8 W/cm$^2$) when the evaporator temperature does not exceed 60 °C. The LHP operating curve is flattened, and two modes of variable conductance and constant conductance are found in the whole tested heat load range [13]. For heat load less than 80 W, the LHP operates at variable conductance mode. The CC temperature is decided by the amount of the subcooling liquid returning from the condenser and the heat leak from the evaporator to the CC if not considering the heat exchange between it and the ambient. The heat leak is nearly compensated by the liquid subcooling and the CC is partly filled with the liquid. The two-phase zone in the condenser increases with increasing heat load, which increases the fraction of the liquid in the CC. The variable conductance mode continues until the CC is completely filled with liquid. For heat load more than 80 W, the LHP operates at constant conductance mode.

For heat load below 80 W, the evaporator temperature difference between the LHP 1 and the LHP 2 is not clear. For heat load greater than 80 W, the evaporator temperature of LHP 2 is lower than that of LHP 1. That means the thermal and hydraulic characteristics of the sample 2 are better than that of the sample 1. On the one hand, the thermal conductivity of the sample 2, which has higher porosity, is lower than that of the sample 1. So the sample 2 is more effective to block the heat leak to the CC. On the other hand, as the pore former content of the sample 2 is more than that of the sample 1, the sample 2 has more large pores from where the generated vapor could easily escape. Meantime, the flow resistance of the liquid supplying for evaporating becomes small.

### 3.3. Thermal resistance

Thermal resistance is calculated in order to assess the thermal performance of the LHP. The total thermal resistance of the LHP is defined as:

$$R_{LHP} = (T_{evap} - T_{cond})/Q \qquad (1)$$

where, $T_{evap}$ is the average temperature of the evaporator, $T_{cond}$ is the average temperature of the condenser, which is calculated by the thermocouples fixed at the condenser inlet (TC 7) and the condenser outlet (TC 8), $Q$ is input power. The uncertainty analysis of $R_{LHP}$ is estimated to be within ±11.6% ($Q < 10$ W) and ±6.4% ($Q > 10$ W).

The total thermal resistances of the LHPs are summarized in the Fig. 4. It shows a typical trend of thermal resistance of the LHP

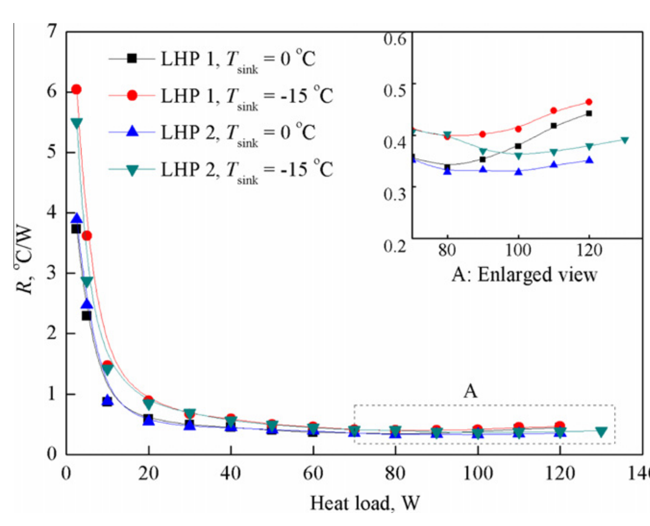


**Fig. 4.** The total thermal resistances of the LHPs.

decreasing with the increase in heat load. But when heat load is greater than 80 W (LHP 1) or 100 W (LHP 2), it increases slightly, as shown in the enlarged view of A zone in Fig. 4. For high heat load, the parasitic heat leak to the CC through the wick becomes huge. Some small bubbles form and coalesce in the wick which could block some paths for transferring the liquid. So the hydraulic characteristic of the wick becomes weak, which decreases the thermal performance of the LHP. The total thermal resistance, if not including the values below 10 W, varies between 1.47 and 0.33 °C/W.

As discussed before, for heat load greater than 80 W, the thermal and hydraulic characteristics of the sample 2 are better than that of the sample 1. Low operating temperature contributes to a small temperature difference between the evaporator and the condenser. So the LHP 2 has lower thermal resistance than the LHP 1.

## 4. Conclusions

In this paper, the thermal performances of the LHPs using different wicks have been analyzed in detail, and the following conclusions can be drawn from the extensive experimental tests as follows.

(1) The thermal and hydraulic characteristics of the sample 2 with porosity of 69% are better than that of the sample 1 with porosity of 65%.
(2) The LHPs could start up at heat load as low as 2.5 W. The maximum heat load which the LHP 1 and the LHP 2 could transfer, respectively, reached 120 W (heat flux 11.8 W/cm$^2$) and 130 W (12.8 W/cm$^2$) when the evaporator temperature did not exceed 60 °C.
(3) The LHPs demonstrated very fast and smooth response to heat load. No obvious temperature oscillation and overshoot phenomena were observed during start-up and steady operation.
(4) The total thermal resistances of the LHPs vary between 1.47 and 0.33 °C/W at heat load ranging from 10 W to 130 W.

## Acknowledgement

The current work was supported by the National Natural Science Foundation of China (Grant Nos. 50876035, 50906026, 51036003).

## References

[1] Y.F. Maydanik, Review: loop heat pipes, Appl. Therm. Eng. 25 (2005) 635–657.
[2] S. Launay, V. Sartre, J. Bonjour, Parametric analysis of loop heat pipe operation: a literature review, Int. J. Therm. Sci. 46 (2007) 621–636.
[3] J. Ku, Operating characteristics of loop heat pipes, SAE Paper No. 1999-01-2007, 1999.
[4] S. Becker, S. Vershinin, V. Sartre, E. Laurien, J. Bonjour, Y.F. Maydanik, Steady state operation of a copper–water LHP with a flat-oval evaporator, Appl. Therm. Eng. 31 (5) (2011) 686–695.
[5] W. Joung, T. Yu, J. Lee, Experimental study on the loop heat pipe with a planar bifacial wick structure, Int. J. Heat Mass Transfer 51 (2008) 1573–1581.
[6] Z.C. Liu, D.X. Gai, H. Li, W. Liu, J.G. Yang, M.M. Liu, Investigation of impact of different working fluids on the operational characteristics of miniature LHP with flat evaporator, Appl. Therm. Eng. 31 (16) (2011) 3387–3392.
[7] D.X. Gai, Z.C. Liu, W. Liu, J.G. Yang, Operational characteristics of miniature loop heat pipe with flat evaporator, Heat Mass Transfer 46 (2009) 267–275.
[8] R. Singh, A. Akbarzadeh, M. Mochizuki, Operational characteristics of the miniature loop heat pipe with non-condensable gases, Int. J. Heat Mass Transfer 53 (2010) 3471–3482.
[9] C.C. Yeh, C.N. Chen, Y.M. Chen, Heat transfer analysis of a loop heat pipe with biporous wicks, Int. J. Heat Mass Transfer 52 (2009) 4426–4434.
[10] Z.Q. Chen, P. Cheng, T.S. Zhao, An experimental study of two phase flow and boiling heat transfer in bi-dispersed porous channels, Int. Commun. Heat Mass Transfer 27 (3) (2000) 293–302.
[11] H. Li, Z.C. Liu, B.B. Chen, W. Liu, C. Li, Development of biporous wicks for flat-plate loop heat pipe, Exp. Therm. Flu. Sci. (2011), doi:10.1016/j.expthermflusci.2011.10.007.
[12] G.M. Xin, K.H. Cui, Y. Zou, L. Chen, Development of sintered Ni-Cu wicks for loop heat pipes, Sci. China Ser. E-Tech. Sci 52 (6) (2009) 1607–1612.
[13] S. Launay, V. Sartre, J. Bonjour, Analytical model for characterization of loop heat pipes, J. Thermophys. Heat Transfer 22 (4) (2008) 623–631.